

Article

A Weighted and Epsilon-Constraint Biased-Randomized Algorithm for the Biobjective TOP with Prioritized Nodes

Lucia Agud-Albesa ¹, Neus Garrido ², Angel A. Juan ^{3,*}, Almudena Llorens ¹ and Sandra Oltra-Crespo ⁴

¹ Department of Applied Mathematics, Universitat Politècnica de València, 03801 Alcoy, Spain; lagudal@mat.upv.es (L.A.-A.); alllopa@upv.edu.es (A.L.)

² Instituto de Matemática Multidisciplinar, Universitat Politècnica de València, 46022 Valencia, Spain

³ Center for Research in Production Management and Engineering, Universitat Politècnica de València, 03801 Alcoy, Spain

⁴ Technological Institute of Informatics, Universitat Politècnica de València, 03801 Alcoy, Spain; soltra@mat.upv.es

* Correspondence: ajuanp@upv.es

Abstract: This paper addresses a multiobjective version of the Team Orienteering Problem (TOP). The TOP focuses on selecting a subset of customers for maximum rewards while considering time and fleet size constraints. This study extends the TOP by considering two objectives: maximizing total rewards from customer visits and maximizing visits to prioritized nodes. The MultiObjective TOP (MO-TOP) is formulated mathematically to concurrently tackle these objectives. A multistart biased-randomized algorithm is proposed to solve MO-TOP, integrating exploration and exploitation techniques. The algorithm employs a constructive heuristic defining biefficiency to select edges for routing plans. Through iterative exploration from various starting points, the algorithm converges to high-quality solutions. The Pareto frontier for the MO-TOP is generated using the weighted method, epsilon-constraint method, and Epsilon-Modified Method. Computational experiments validate the proposed approach's effectiveness, illustrating its ability to generate diverse and high-quality solutions on the Pareto frontier. The algorithms demonstrate the ability to optimize rewards and prioritize node visits, offering valuable insights for real-world decision making in team orienteering applications.

Keywords: team orienteering problem; heuristics; biased-randomized algorithms; multiobjective optimization; Pareto frontier



Citation: Agud-Albesa, L.; Garrido, N.; Juan, A.A.; Llorens, A.; Oltra-Crespo, S. A Weighted and Epsilon-Constraint Biased-Randomized Algorithm for the Biobjective TOP with Prioritized Nodes. *Computation* **2024**, *12*, 84. <https://doi.org/10.3390/computation12040084>

Academic Editor: Demos T. Tsahalis

Received: 14 March 2024

Revised: 15 April 2024

Accepted: 17 April 2024

Published: 20 April 2024



Copyright: © 2024 by the authors. Licensee MDPI, Basel, Switzerland. This article is an open access article distributed under the terms and conditions of the Creative Commons Attribution (CC BY) license (<https://creativecommons.org/licenses/by/4.0/>).

1. Introduction

The TOP was introduced by Chao et al. [1] as a multivehicle extension of the Orienteering Problem (OP) described in Golden et al. [2], and it has many applications in different areas, such as smart cities, humanitarian logistics, or military logistics [3]. One of the main differences between the TOP and the popular vehicle routing problem (VRP) is that the former does not require visiting all customers due to the fixed size of the fleet of vehicles. Also, in the case of the TOP, the focus is on maximizing the total reward collected by visiting customers, while the capacity constraint is centered on the maximum travel time per route instead of on the loading characteristics of each vehicle in the fleet. Also, while in the VRP it is usually assumed that the origin and the destination depots are represented by the same node, in the case of the TOP, it is usual to assign each depot to a different node. In this paper, a variant of the classical TOP is considered by introducing two different types of nodes: prioritized nodes (PN) and nonprioritized nodes. They are represented in Figure 1 with triangles and circles, respectively.

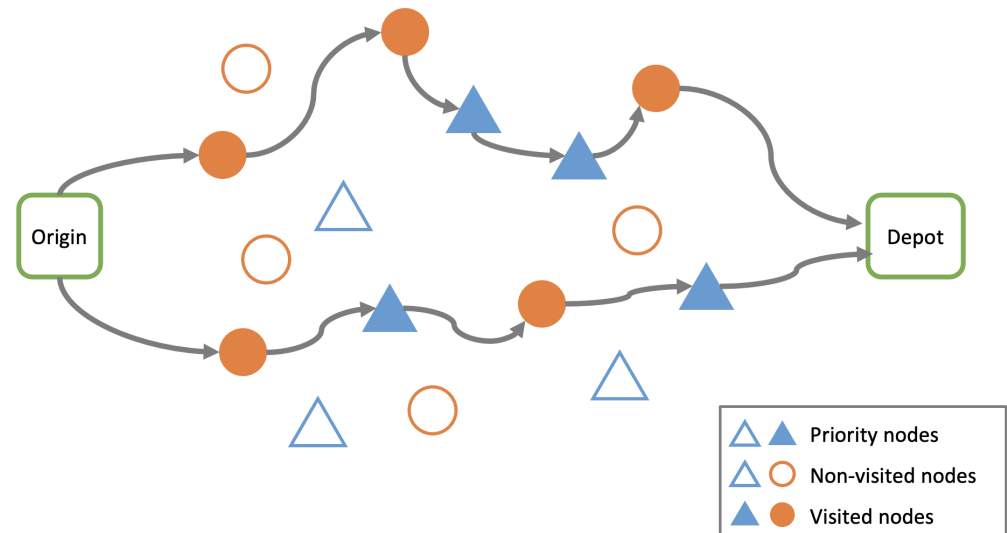


Figure 1. A basic schema of the multiobjective TOP considered in this paper.

One of the restrictions to take into account is the maximum length or duration of any route. The goal in the classical TOP is to maximize the total reward obtained when visiting a collection of nodes of the initial set using the available fleet of vehicles. The total reward is reached by the sum of the rewards of each of the routes that constitute the total solution. In general, the travel times and the rewards are deterministic variables. A wide range of examples can be considered as a deterministic TOP; hence, the existing literature for this kind of deterministic study is very extensive [4]. In addition to the introduction of prioritized nodes in the original TOP, the main contribution of this work is the proposal of a novel methodology that allows us to optimize both the rewards obtained from the nodes visited and the number of prioritized nodes visited. In order to achieve this goal, the proposed methodology combines biased-randomized heuristics with the epsilon-constraint method.

The rest of this paper is structured as follows: Section 2 provides a review of the classical TOP. Section 3 introduces a formal definition of the deterministic TOP, and then more details are given on the specific MO-TOP analyzed in this work. Section 4 describes three solution approaches that have been applied to solve the mathematical model introduced in the previous section. The computational experiments and the final results are described in Section 5. Finally, conclusions and future lines are summarized in Section 6.

2. Related Work

Vansteenwegen et al. [5] conducted an extensive review that thoroughly investigates the Orienteering Problem, including several of its variants. Their analysis shows the predominant themes in the existing literature, primarily revolving around practical applications such as technician routing, city logistics, athlete recruitment, and military logistics. These applications demand efficient problem-solving approaches. However, the review raises concerns regarding the current solving methodologies, noting their time-consuming nature, particularly when dealing with large-scale instances. While previous research on the TOP primarily leans towards deterministic versions, it fails to address the uncertainties inherent in real-world scenarios, including varying weather conditions and unexpected road obstacles. Hence, Panadero et al. [6] discuss a more realistic approach, suggesting the utilization of historical data to model random elements within the system. This can be achieved through the incorporation of best-fit probability distributions or empirical ones. Only a limited number of prior studies have ventured into stochastic versions of TOP, integrating optimization with simulation techniques [7]. The scientific literature predominantly focuses on deterministic versions of the TOP. For example, Archetti et al. [8]

tackle the TOP using various algorithms, such as a generalized tabu search and a variable neighborhood search algorithm. Their experiments reveal that the latter yields superior results. Similarly, Ke et al. [9] introduce an ant colony optimization algorithm for the TOP, highlighting the advantages of combining different randomized methods to expedite the discovery of near-optimal solutions. Vansteenwegen et al. [10] propose a guided local search, emphasizing the importance of diversification procedures to enhance solutions. In a different research line, Vansteenwegen et al. [11] introduce an iterated local search meta-heuristic for the TOP with time windows, achieving solutions with a narrow average gap of 1.8% compared with established benchmarks. Souffriau et al. [12] approach the TOP with a path relinking heuristic, resulting in promising outcomes with a tiny average gap of 0.04% relative to benchmarks.

In a distinct context, Tricoire et al. [13] explore the multiperiod TOP, integrating a variable neighborhood search algorithm with an exact algorithm. These authors address the classic TOP and compare their solutions with benchmark results, achieving solutions with an average gap of 1.0%. Souffriau et al. [14] tackle the TOP by combining an iterated local search framework with a greedy randomized adaptive search procedure, resulting in solutions with an average gap of 5.2% with respect to benchmark results. Verbeeck et al. [15] explore the time-dependent OP and propose an algorithm merging ant colony optimization principles with a time-dependent local search algorithm, providing solutions with a minimal gap of 1.4%. Meanwhile, Vidal et al. [16] focus on a vehicle routing problem closely related to the TOP, introducing a neighborhood search approach that yields solutions with an average gap of merely 0.1%. They also emphasize the advantages of hybrid solving approaches. Paolucci et al. [17] present a hybrid problem combining a vehicle routing problem with the TOP, aiming to optimize location-allocation for maximum rewards. Their approach involves a cluster-first and route-second decomposition, enhanced by variable neighborhood search incorporating a simulated annealing acceptance rule. Estrada-Moreno et al. [18] address a biobjective TOP with a soft constraint related to driving range, employing a biased-randomized algorithm penalizing routes exceeding the range. This approach outperforms other methods for a hard-constrained TOP. Ruiz-Meza et al. [19] apply the TOP in the tourism industry, concentrating on crafting group routes to maximize traveler preferences. They propose metaheuristics for problem resolution and compare results derived from an exact method. Likewise, Sankaran et al. [20] explore the TOP with multiple depots, presenting an attention-based model for resolution. Their approach is validated through comparisons with various reconnaissance scenarios, showing the efficacy of their data generation methodology when juxtaposed against heuristics, machine learning, and exact solvers. Similarly, Panadero et al. [21] propose a simheuristic algorithm for solving a stochastic TOP and perform a set of experiments to show that their approach outperforms the standard sample average approximation method.

Other authors have conducted studies in different fields using multiobjective functions to achieve their objectives. Wattanasang and Ransikarbum [22] have two objectives: an economic one (associated with utility distances between plant locations) and a risk-based cost objective for locating plants within an industrial park. Mohammadi et al. [23] aim to suggest an optimal configuration for an intelligent supply chain handling multiple perishable products, employing a vendor-managed inventory strategy augmented by IoT technologies. This approach aims to overcome the hurdles typically encountered in conventional supply chains. For that reason, they have objective function total costs and delivery times. Ref. [24] introduce a biobjective mixed-integer linear model addressing the vaccine distribution chain problem. It concurrently accounts for economic and social objectives. Also, in the field of tourism and maritime supply chains, there are recent studies, as can be seen in Shojatalab et al. [25] and Elmi et al. [26], both using an epsilon-constraint approach. A myriad of challenges across diverse domains, including those previously elucidated and the one under consideration in this study, necessitate the concurrent optimization of multiple objectives or goals. In the study conducted by Banerjee et al. [27], metaheuristic algorithms exhibited their robustness and efficacy in addressing challenges associated with

multiobjective optimization. Various multiobjective optimization techniques are employed, including the weighted sum approach and the epsilon-constraint technique. In the context of the wireless body area network (WBAN), Memarian et al. [28] present a reactive routing protocol for WBANs that combines a fuzzy heuristic with a metaheuristic learning model.

3. Formal Description of the MultiObjective TOP

In this section, we consider the mathematical model of the deterministic TOP and extend the model to a MultiObjective TOP. As previously stated, the goal of the MO-TOP is to find the visiting routes that maximize both the rewards obtained from each visited node and the total number of priority nodes considered, simultaneously. Obviously, the number of finding routes depends on the number of available vehicles. The presented model is based on the formulation proposed in Evers et al. [29] (please refer to the summary table of nomenclatures located at the end of this article). The network is characterized by a directed graph $G = (N', E)$, consisting of N' nodes and E edge connections. N' is composed of the origin depot (node 0), the destination depot (node $n + 1$), and the intermediate nodes denoted as $N = \{1, 2, \dots, n\}$, so $N' = \{0, 1, 2, \dots, n + 1\}$. E represents the set of connection edges between these nodes and it is defined as $E = \{(i, j) / i, j \in N', i \neq j\}$. Within this framework, we define a set D , comprising homogeneous vehicles. Each vehicle, represented as $d \in D$, embarks on its journey from the origin depot, provides services to designated intermediate nodes, and ultimately concludes its route at the destination depot.

In the deterministic formulation of the TOP, it is common to assume that the travel time for each edge is a positive constant, i.e., $t_{ij} = t_{ji} > 0, \forall i, j \in N$. Through this work, the Euclidean distance between nodes i and j is used as an estimate for this time. Notice that each vehicle sets out on its route and can only serve specific nodes due to a constraint on maximum travel time, t_{max} . Moreover, each vehicle must reach the destination depot within the allocated travel time. The act of servicing the intermediate nodes during the initial pass leads to the acquisition of a reward, symbolized as $u_i \geq 0$. Note that the origin and the destination depots do not yield any associated rewards. For every edge $(i, j) \in E$ and each vehicle $d \in D$, we introduce binary variables x_{ij}^d , which take on a value of 1 if vehicle d traverses edge (i, j) and 0 otherwise. Additionally, we introduce the variable y_i^d to indicate the position of node i in the tour made by vehicle d and consider the binary variable z_i , which is equal to 1 if node i is priority and 0 if it is not priority. Based on these definitions, a mathematical model of the deterministic MO-TOP is given next:

$$\begin{cases} \max \sum_{d \in D} \sum_{(i,j) \in E} u_j x_{ij}^d \\ \max \sum_{d \in D} \sum_{(i,j) \in E} z_j x_{ij}^d \end{cases} \quad (1)$$

$$\text{s.t. } \sum_{d \in D} \sum_{i \in N'} x_{ij}^d \leq 1 \quad \forall j \in N \quad (2)$$

$$y_i^d - y_j^d + 1 \leq (1 - x_{ij}^d) |N| \quad \forall i, j \in N, \forall d \in D \quad (3)$$

$$\sum_{(i,j) \in E} t_{ij} x_{ij}^d \leq t_{max} \quad \forall d \in D \quad (4)$$

$$\sum_{i \in N'} x_{ij}^d = \sum_{h \in N'} x_{jh}^d \quad \forall d \in D, \forall j \in N \quad (5)$$

$$\sum_{j \in N} x_{0j}^d = 1 \quad \forall d \in D \quad (6)$$

$$\sum_{j \in N} x_{jn+1}^d = 1 \quad \forall d \in D \quad (7)$$

$$y_j^d \geq 0 \quad \forall j \in N, \forall d \in D \tag{8}$$

$$x_{ij}^d \in \{0, 1\} \quad \forall i, j \in E, \forall d \in D \tag{9}$$

$$z_j \in \{0, 1\} \quad \forall j \in N \tag{10}$$

Equation (1) represents the multiobjective function aimed at maximization. Constraints (2) guarantee that each node is serviced no more than once. Constraints (3) act as a preventive measure against the formation of sub-tours. Constraints (4) stipulate that the total travel time for each vehicle must not exceed its predetermined threshold. Constraints (5) serve as a balance constraint for the flow, ensuring that any arrival at a node must be offset by a departure. Constraints (6) and (7) specify that all vehicles must initiate their journeys from the original depot (node 0), and subsequently, after traversing their routes, arrive at the destination depot (node $n + 1$). Lastly, constraints (8)–(10) show the characteristics and implications of the variables y_j^d , x_{ij}^d , and z_j .

4. Alternative Approaches for Solving the MO-TOP

In this paper, several alternative ways to solve the MultiObjective TOP described above are introduced: the Weighted Average Method (WAM), the Ponderate Weighted Average Method (POWAM), the epsilon-constraint method (ECM), and the Epsilon-Modified Method (EMM). Their main characteristics and algorithms are described below.

4.1. The Weighted Average Method and the Ponderate Weighted Average Method

This subsection provides the general framework of the WAM (Algorithm 1) to solve the MO-TOP and the weight considered in the objective function for obtaining the POWAM. This method is extensively employed in the optimization of multiobjective functions. The objective is to discover solutions that meet various criteria, and the weighted average serves as a prevalent technique for amalgamating these criteria into a unified aggregated objective function. The fundamental concept behind the weighted average entails assigning a weight to each objective, thereby representing its relative significance in the decision-making process. Subsequently, a comprehensive score is computed for each solution by multiplying the values of the objectives by their respective weights and then summing them. The Weighted Average Method proves especially valuable when tackling optimization problems where it is unfeasible to identify a singular solution that concurrently optimizes all objectives. Instead, it empowers decision-makers to ascertain solutions that adeptly strike a balance among the diverse objectives, taking into account their preferences and constraints. As mentioned earlier, the considered objective function aims to maximize both rewards and the number of priority nodes visited. Hence, it can be represented as a biobjective function. This function is constructed through a normalized convex linear combination, as expressed in Equation (11) below:

$$\max \sum_{d \in D} \sum_{(i,j) \in A} \lambda \eta u_j x_{ij}^d + (1 - \eta) z_j x_{ij}^d, \quad \eta \in [0, 1], \quad \lambda \in \mathbb{R}. \tag{11}$$

The constraints have been previously described in Equations (2) to (10). Notice that the real factor λ in Equation (11) depends on the magnitude of the rewards considered in the instances. Normalizing the rewards in the biobjective function ensures that the quantities to be compared fall within a similar range, and therefore, one does not weight more than the other. In particular, for $\lambda = 1$, the WAM is obtained, while for other values of λ , the POWAM is taken.

We initiate the solution-finding process by employing a constructive heuristic. Given the intricacies of the TOP problem, this heuristic accounts for the following factors: (i) the origin and destination nodes may not be the same; (ii) there is no strict requirement to visit all nodes; (iii) there are priority nodes which should be visited; and (iv) the construction of the routing plan takes into consideration not just time or distance savings but also the collected rewards. Hence, the heuristic starts by generating an initial ‘dummy’

solution, where each location is connected to both the origin and destination depots. Subsequently, these dummy routes undergo an iterative merging process. During this phase, the heuristic seeks to combine routes as much as possible while ensuring that the total travel time for each route remains within the defined threshold. To facilitate route merging in the original algorithm, a list of potential merging edges is created, sorted in descending order of efficiency. The efficiency associated with an edge (i, j) is computed as $e_{ij} = \alpha \cdot s_{ij} + (1 - \alpha) \cdot (u_i + u_j)$, where $s_{ij} = t_{i(n+1)} + t_{0j} - t_{ij}$ represents the time-based savings obtained with the merge, and $u_i + u_j$ reflects the combined reward from nodes i and j . Note that in the POWAM, the efficiency was considered with already weighted data. The parameter α , falling within the range $[0, 1]$, is contingent on the diversity of rewards among nodes and necessitates empirical fine-tuning. In scenarios with substantial reward diversity, α tends to approach zero, while in more homogeneous scenarios, α gravitates toward one. To determine the optimal α for each scenario, the constructive heuristic is executed 21 times, with α ranging from 0 to 1 in increments of step 0.05 during each iteration. Once this merging process is completed, an initial solution is obtained. The core idea of the WAM is to introduce a new criterion to sort the initial edges list according to efficiency values and priority nodes for each value of $\eta \in [0, 1]$ with increments of 0.05. For this purpose, the biefficiency values are defined by

$$b_{ij} = \gamma e_{ij} + (1 - \gamma)(z_i + z_j), \quad \gamma \in [0, 1], \quad (12)$$

where γ runs in the same way as α . The optimal α and γ are determined experimentally by choosing the ones that provide the greater value of the biobjective function. Then, the constructive heuristic is executed for each value of η . The initial solution is established when the merging process is completed. Now, by systematically examining solutions from different starting points, the algorithm converges towards a refined set of high-quality solutions using a biased-randomized algorithm [30]. In the end, a near-optimal (or at least high-quality) solution is provided. This solution returns both the rewards and the priority nodes visited on those routes. The Algorithm 1 illustrates the main steps of the WAM-based code. Notice that, for values of $\gamma = 1$ in Equation (12), the usual efficiency list in the constructive algorithm is obtained, while for $\eta = 1$ or $\eta = 0$ in Equation (11), the multiobjective function is simplified as a single-objective function. Moreover, for $\eta = \lambda = 1$ the multiobjective function is the usual function to maximize in the TOP. Therefore, running the new algorithm implemented here gives the same results.

Hence, the proposed algorithm aims to find a good solution for each value of η in Equation (11). To achieve this, the algorithm runs α and γ a total of 21 times from 0 to 1, generating the best solution experimentally for each combination of α and γ . This process involves sorting the biefficiency list for each combination, allowing for the exploration of different approximations to the solution during the merging process. Once a solution maximizing the objective function for each η is obtained, the algorithm proceeds (from line 13 to the end) to further improve it using a multistart biased-randomized algorithm. This improvement is achieved by temporarily changing the biefficiency list for a while (elapsed-time), ultimately returning the best solution (Best_Sol). Note that each time a solution is constructed, the algorithm identifies all possible routes that comply with the imposed restrictions starting from the dummy solution. These routes are then sorted based on the total biobjective value obtained from each one. Finally, the solution is constructed by selecting as many routes as the fleet size allows. Additionally, notice that the only distinction between the POWAM and the WAM approaches lies in the consideration of reward values, whether weighted or not, respectively.

Algorithm 1 WAM/POWAM

Input: Data
Output: Best_Sol

```

1: for  $\eta = 0 : 0.05 : 1$  do
2:   initialize(Best_Sol)
3:   for  $\gamma = 0 : 0.05 : 1$  do
4:     for  $\alpha = 0 : 0.05 : 1$  do
5:       generate and sort bi-efficiency list
6:        $Sol \leftarrow merging(\text{dummy solution})$ 
7:       if  $Sol(\text{bi-objective}) > Best\_Sol(\text{bi-objective})$  then
8:          $Best\_Sol \leftarrow Sol, \alpha, \gamma$ 
9:       end if
10:    end for
11:  end for
12:  while  $elapsed \leq test.maxTime$  do
13:    New_Sol  $\leftarrow$  update(BRA,bi-efficiency list)
14:    if  $New\_Sol(\text{bi-objective}) > Best\_Sol(\text{bi-objective})$  then
15:      Best_Sol  $\leftarrow$  New_Sol
16:    end if
17:  end while
18:  return Best_Sol
19: end for
20: end

```

4.2. The Epsilon-Constraint Method

The epsilon-constraint method (ECM, Algorithm 2) is a powerful technique employed in multiobjective optimization to address decision-making problems with conflicting objectives [25,26]. In the field of optimization, the challenge lies in identifying solutions that offer a balanced trade-off among multiple objectives. The ECM facilitates the transformation of a multiobjective problem into a single-objective problem by introducing supplementary constraints. This method involves designating one objective as the primary focus and treating the remaining objectives as constraints. The term ‘epsilon’ denotes a small positive value that defines the acceptable deviation from the optimal value for the secondary objectives. In the ECM, one objective function is maximized, in this case the rewards, and the total priority nodes visited are counted and stored. Then, this initial objective function is again maximized while the other objective function, the priority nodes visited, becomes a constraint where the value counted initially must be exceeded by a certain quantity (ϵ). It should be noted that both optimization problems have been solved with the aforementioned algorithm. Despite optimizing the same single-objective function in both cases (rewards), the bi-efficiency list is used to construct the solutions. In order to determine the optimal α and γ related to the bi-efficiency list, we follow the same process explained previously. However, the solutions to both problems have not been constructed following the same criteria even though in both cases the rewards are maximized. While in the first step the bi-efficiency list selected is the one that generates the highest rewards, in the second step, the list that provides the highest number of priority nodes visited is taken. In the first step, the objective function is given by

$$\max \sum_{d \in D} \sum_{(i,j) \in A} u_j x_{ij}^d$$

subject to the constraints described in Equations (2) to (10). The NP value of this solution is stored, $PN^* = \sum_{d \in D} \sum_{(i,j) \in A} u_j z_{ij}^d$. Also, in the second part, the objective function is the same,

with the constraints mentioned above but adding a new one:

$$\sum_{d \in D} \sum_{(i,j) \in A} u_j z_{ij}^d \geq PN^* + \epsilon, \tag{13}$$

where ϵ ranges from 0 to $\max \sum_{d \in D} \sum_{(i,j) \in A} u_j z_{ij}^d - PN^*$ for saving computational cost.

Algorithm 2 ECM

```

Input: Data
Output: Best_Sol
1: initialize(Best_Sol_1)
2: for  $\gamma = 0 : 0.05 : 1$  do
3:   for  $\alpha = 0 : 0.05 : 1$  do
4:     generate and sort bi-efficiency list
5:      $Sol\_1 \leftarrow merging(\text{dummy solution})$ 
6:     if  $Sol\_1(\text{reward}) > Best\_Sol\_1(\text{reward})$  then
7:        $Best\_Sol\_1 \leftarrow Sol\_1, \alpha, \gamma$ 
8:     end if
9:   end for
10: end for
11: while  $elapsed \leq test.maxTime$  do
12:    $New\_Sol\_1 \leftarrow update(\text{BRA}, \text{bi-efficiency list})$ 
13:   if  $New\_Sol\_1(\text{reward}) > Best\_Sol\_1(\text{reward})$  then
14:      $Best\_Sol\_1 \leftarrow New\_Sol\_1$ 
15:   end if
16: end while
17: initialize(Best_Sol_2)
18: for  $\gamma = 0 : 0.05 : 1$  do
19:   for  $\alpha = 0 : 0.05 : 1$  do
20:     generate and sort bi-efficiency list
21:      $Sol\_2 \leftarrow merging(\text{dummy solution})$ 
22:     if  $Sol\_2(PN) > Best\_Sol\_2(PN)$  then
23:        $Best\_Sol\_2 \leftarrow Sol\_2, \alpha, \gamma$ 
24:     end if
25:   end for
26: end for
27: while  $elapsed \leq test.maxTime$  do
28:    $New\_Sol\_2 \leftarrow update(\text{BRA}, \text{bi-efficiency list})$ 
29:   if  $New\_Sol\_2(PN) > Best\_Sol\_2(PN)$  then
30:      $Best\_Sol\_2 \leftarrow New\_Sol\_2$ 
31:      $maxPN \leftarrow Best\_Sol\_2(PN)$ 
32:   end if
33: end while
34: for  $\epsilon = 0 : 1 : maxPN$  do
35:   initialize(Best_Sol)
36:   for  $\gamma = 0 : 0.05 : 1$  do
37:     for  $\alpha = 0 : 0.05 : 1$  do
38:       generate and sort bi-efficiency list
39:        $Sol\_3 \leftarrow merging(\text{dummy solution})$ 
40:       if  $Sol\_3(PN) > Best\_Sol(PN) \& Sol\_3(PN) \geq Sol\_1(PN) + \epsilon$  then
41:          $Best\_Sol \leftarrow Sol\_3, \alpha, \gamma$ 
42:       end if
43:     end for
44:   end for
45:   while  $elapsed \leq test.maxTime$  do
46:      $New\_Sol\_3 \leftarrow update(\text{BRA}, \text{biefficiency list})$ 
47:     if  $New\_Sol\_3(\text{reward}) > Best\_Sol(\text{reward}) \text{ and } New\_Sol\_3(PN) \geq Sol\_1(PN) + \epsilon$  then
48:        $Best\_Sol \leftarrow New\_Sol\_3$ 
49:     end if
50:   end while
51:   return Best_Sol
52: end for
53: end

```

The main structure is shown in Algorithm 2 and described next. In the first step (from line 2 to line 16), the constructive algorithm by Panadero et al. [31] is used to optimize the rewards of the visited nodes. Similar to the previous algorithm, it searches for the combination of α and γ whose associated biefficiency list obtains the maximum rewards

on the proposed routes. From this solution, better approximations are sought using a multistart biased-randomized algorithm, where the biefficiency list is rearranged during a period (from line 17 to 33). Next, the maximum number of priority nodes that can be visited ($maxPN$) is obtained using the same constructive algorithm (from lines 34 to 51). This value is determined to ensure that the algorithm does not perform unnecessary iterations. Finally, the best approximation to the solution is built, providing both rewards and priority node values. For each value of ϵ between 0 and $maxPN$, solutions are obtained. The coefficients that provide the biefficiency list ensuring a higher reward for each ϵ are determined. Among these solutions that verify the ϵ constraint, the one that provides the highest reward is retained. This solution is further improved with a multistart biased-randomized algorithm, where the biefficiency list is reordered.

Two ways are developed to ensure that the epsilon-constraint is verified:

- Epsilon-Constraint Positional Method (ECPM): The procedure to generate a solution that satisfies the new constraint where ϵ is involved starts by constructing a list of routes ordered by reward. Then, the list is separated into two: one auxiliary solution of the fleet size and the other with the rest of the routes. The auxiliary solution will be the solution of the problem in case it verifies the constraint. Otherwise, the one with the lowest reward is replaced by one of the rest that has a higher PN than it. Recursively, all the positions of the auxiliary solution are run through until a solution is found or the list has been completed.
- Epsilon-Constraint Sublists Method (ECSM): In this other implementation, once the above list of routes has been constructed, the possible sublists of fleet size are generated. Of all of them, the one with the highest reward that verifies the restriction is chosen.

The solutions given by these approaches for solving the MO-TOP lead to different results, as shown in Section 5.

4.3. The Epsilon-Modified Method

Based on the Absolute Priority (Lexicographic) Method, the Epsilon-Modified Method (EMM, Algorithm 3) described in this section is structured in two steps as independent problems. Firstly, the rewards are considered as the objective function. In the second problem, the priority nodes constitute the new objective function, and the reward achieved in the first step is added as a new constraint that we will relax when the value of epsilon increases. In the context of the multiobjective optimization problem being considered, the EMM is applied as follows: first, a single-objective constructive algorithm is applied to maximize only the rewards, while the total visited priority nodes in the provided solution are counted. Subsequently, a reformulation of the previous algorithm is applied to maximize the visited priority nodes with a new ϵ -constraint. The added constraint involves the reward of the new solution that must be higher than the previous reward unless by a certain quantity ϵ , which varies between 0 and the previous reward. As in the ECM, in the first step, the objective function is given by

$$\max \sum_{d \in D} \sum_{(i,j) \in A} u_j x_{ij}^d$$

subject to the same constraints described above. However, in the second part, the objective function is

$$\max \sum_{d \in D} \sum_{(i,j) \in A} u_j z_{ij}^d$$

adding the following constraint:

$$\sum_{d \in D} \sum_{(i,j) \in A} u_j x_{ij}^d \geq \max \sum_{d \in D} \sum_{(i,j) \in A} u_j x_{ij}^d - \epsilon, \tag{14}$$

where ε ranges from 0 to $\max_{d \in D} \sum_{(i,j) \in A} u_j x_{ij}^d$. In both steps of the EMM, the biefficiency list is considered with the same purpose. An optimal solution for each ε is obtained through 21 executions. Notice that, while the objective in the first part is to maximize the total reward obtained by visiting the nodes, the structure of the algorithm remains the same as in the epsilon-constraint method. The difference lies in how the solutions are obtained in the second part. For each value of ε between 0 and the maximum value of the reward calculated before with 21 iterations, the constructive algorithm is used again to maximize the number of priority nodes visited. As long as the solution obtained verifies the ε constraint, we use a multistart biased-randomized algorithm to reorder the biefficiency list, ensuring that these new solutions satisfy the added restriction. The best solution is then returned.

Algorithm 3 EMM

Input: Data
Output: Best_Sol

- 1: initialize(Best_Sol_1)
- 2: **for** $\gamma = 0 : 0.05 : 1$ **do**
- 3: **for** $\alpha = 0 : 0.05 : 1$ **do**
- 4: generate and sort bi-efficiency list
- 5: $Sol_1 \leftarrow merging(\text{dummy solution})$
- 6: **if** $Sol_1(\text{reward}) > Best_Sol_1(\text{reward})$ **then**
- 7: $Best_Sol_1 \leftarrow Sol_1, \alpha, \gamma$
- 8: **end if**
- 9: **end for**
- 10: **end for**
- 11: **while** $elapsed \leq test.maxTime$ **do**
- 12: $New_Sol_1 \leftarrow update(BRA, \text{bi-efficiency list})$
- 13: **if** $New_Sol_1(\text{reward}) > Best_Sol_1(\text{reward})$ **then**
- 14: $Best_Sol_1 \leftarrow New_Sol_1$
- 15: **end if**
- 16: **end while**
- 17: **for** $\varepsilon = 0 : Best_Sol_1(\text{reward})$ **do**
- 18: initialize(Best_Sol)
- 19: **for** $\gamma = 0 : 0.05 : 1$ **do**
- 20: **for** $\alpha = 0 : 0.05 : 1$ **do**
- 21: generate and sort bi-efficiency list
- 22: $Sol \leftarrow merging(\text{dummy solution})$
- 23: **if** $Sol(PN) > Best_Sol(PN) \& Sol(\text{rewards}) \geq Sol_1(\text{reward}) - \varepsilon$ **then**
- 24: $Best_Sol \leftarrow Sol, \alpha, \gamma$
- 25: **end if**
- 26: **end for**
- 27: **end for**
- 28: **while** $elapsed \leq test.maxTime$ **do**
- 29: $New_Sol \leftarrow update(BRA, \text{bi-efficiency list})$
- 30: **if** $New_Sol(PN) > Best_Sol(PN) \text{ and } New_Sol(\text{reward}) \geq Sol_1(\text{reward}) - \varepsilon$ **then**
- 31: $Best_Sol \leftarrow New_Sol$
- 32: **end if**
- 33: **end while**
- 34: **return** Best_Sol
- 35: **end for**
- 36: **end**

5. Computational Experiments

A comprehensive overview of the numerical instances addressed through the five previously mentioned approaches is shown in this section. The aim is to assess and compare

the set of obtained solutions. All the algorithms were programmed in Python and run on a workstation with an Intel Core i5-11400 11th Generation and 32 GB of RAM. The maximum computational time for solving each instance is limited to 200 s. To assess the effectiveness of the proposed solution methods for the TOP, we extended to the biobjective case the widely used benchmark introduced by Chao et al. [1]. This benchmark is a standard choice in the literature for evaluating algorithms designed to address the classical version of the TOP. It is categorized into seven subsets, totaling 320 instances in total, each identified by the nomenclature $pa.b.c$. Here, a denotes the subset identifier, b signifies the number of vehicles, and c represents the maximum driving range. In our experiments, we choose three of the seven subsets and add a new attribute to each instance related to the priority of the node. This is performed by selecting as a ‘prioritized node’ one out of three nodes in the list of nodes. Moreover, when tackling instances that share the same network, our selection was given to those with the greatest number of available vehicles, exactly $b = 4$ vehicles. We exclusively considered instances possessing a ‘sufficient’ driving range, ensuring the capability to reach the farthest node in each instance. This selection strategy guarantees a diverse and representative set of scenarios for a comprehensive evaluation of the proposed solution approaches.

In a multiobjective optimization scenario, distinct, and sometimes competing, objectives must be optimized simultaneously. The primary aim is to discover a set of solutions representing Pareto optimal solutions, i.e., solutions where no single objective can be enhanced without compromising another. The solutions obtained for each instance are shown using a Pareto frontier for the different values of the coefficient η employed in the case of the POWAM and the WAM (Equation (11)), the different values of ε considered in the ECM (Equation (13)), and the EMM (Equation (14)). The abscissa axis represents the reward obtained and the ordinate axis represents the number of priority nodes visited. From the Pareto frontier, the decision-maker will be able to select the best solutions according to his/her utility function, taking into account the combination of reward values and priority nodes visited. As expected, the achieved reward decreases as more prioritized nodes are forced to be visited in the solution and vice versa. Notice that the first example, p4.4.c, has a total of 100 nodes, including the two depots, from which 33 are prioritized nodes. Similarly, the second instance, p5.4.c, has a total of 66 nodes, including depots, from which 21 are prioritized. The last instance, p7.4.c, has 102 total nodes, and 34 of them are priority nodes. For each instance, parameter c was varied in two ways, where the unique difference between cases is $tmax$, where $tmax$ is the maximum time allowed by each vehicle in the fleet to complete a route.

In order to illustrate the routes traveled in each of the solutions obtained, the following graphs are presented. Specifically, for instance, for p5.4.r, we display the routes obtained with the EMM for $\varepsilon = 43$ and $\varepsilon = 129$, corresponding to the restriction (14), in Figure 2. Additionally, routes related to the POWAM are depicted in Figure 3 for $\eta = 0.1$ and $\eta = 0.5$ in Equation (11).

The WAM and the POWAM were executed with $\lambda \in 0.1, 1$, corresponding to the normalized (POWAM) and not-normalized (WAM) biobjective functions, respectively. One of the purposes of reward weighting is to balance the two elements that form the multiobjective function. Tables 1–3 display the numerical results for some of the selected examples. For each instance and method, the obtained reward and the PN are shown for the solution corresponding to each η or ε . These solutions are also represented in Figures 4–9. Additionally, the Pareto frontiers, which consist of the best solutions regardless of the method, are highlighted in red. Specifically, Figures 4 and 5 pertain to the results in Table 1, Figures 6 and 7 correspond to Table 2, and Figures 8 and 9 depict the results in Table 3.

The main purpose of this work is to provide a framework for comparing five different multiobjective approaches. Let us remark that when looking at the Pareto frontiers, all five methods provide, at least in some of the examples, the best solution. Note that the extreme values of the frontiers could be assimilated as solutions to single-objective optimization problems. The points located on the left side of the graphs maximize the total number

of prioritized nodes visited, while those on the right side maximize the total reward. It can be observed that the ECSM contributes more to the Pareto frontier of examples p7.4.c (Figures 8 and 9), whose fundamental difference with respect to the other examples is that the maximum time per route is greater and the distribution of the nodes in the XY plane is more uniform. However, in the examples corresponding to p5.4.c, whose route time is the smallest of the examples studied, the POWAM is the one that provides the best results and therefore the one that contributes the most points to the Pareto frontier in Figures 6 and 7. Finally, in Figures 4 and 5, it is observed that all methods contribute to the Pareto frontiers, with the exception of ECSM, which might require a longer routing time. As a consequence, we cannot determine a dominant method with respect to the others, as they all contribute to the Pareto frontiers of the different examples. Therefore, it is up to the user to choose the method to be used depending on the objectives to be achieved. Furthermore, for a better comprehension of the variability of the results with the different methods here implemented, the values are shown by the box plots in Figures 10 and 11. To facilitate the visualization of the data distribution, the values of rewards and priority nodes visited are shown separately in Figures 10 and 11, respectively. Example p4.4.o. is taken as a reference, being the results obtained with the other examples similar.

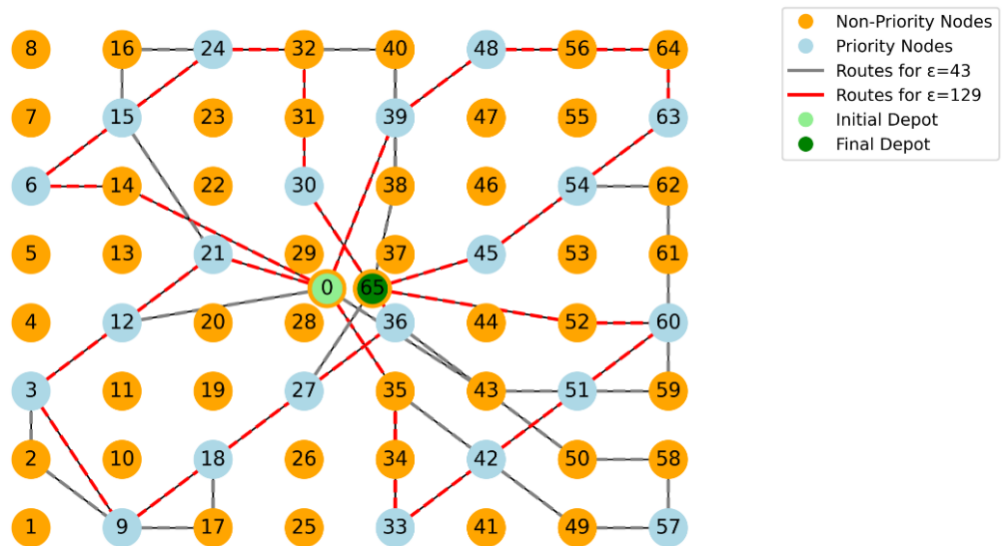


Figure 2. Graph for the instance p5.4.r with the EMM.

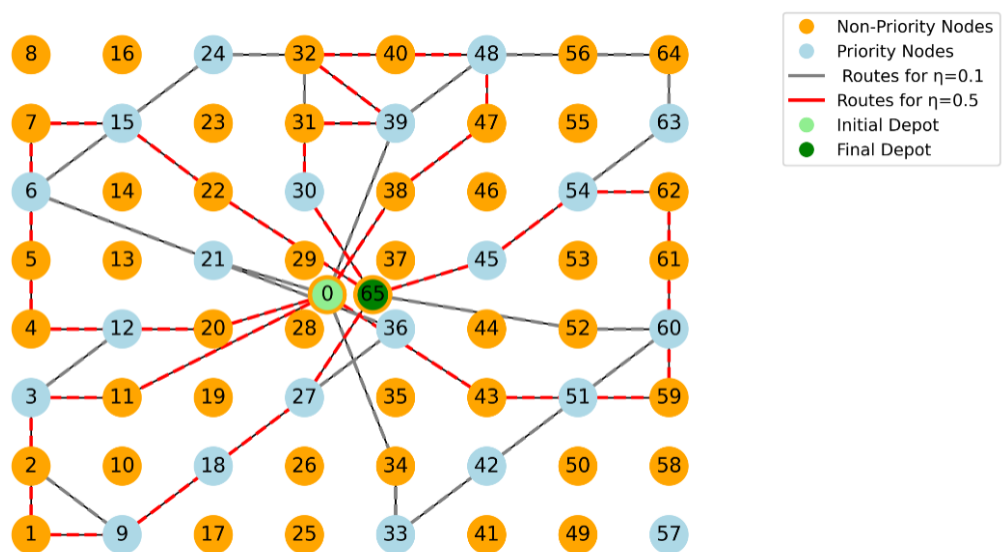


Figure 3. Graph for the instance p5.4.r with the POWAM.

Table 1. Numerical results of instances p44o and p44r.

Instance p44o									
Reward_WAM	P_nodes_WAM	Reward_POWAM	P_nodes_POWAM	Reward_EMM	P_nodes_EMM	Reward_ECPM	P_nodes_ECPM	Reward_ECSCM	P_nodes_ECSCM
500	28	447	31	840	19	650	14	702	18
805	21	481	31	778	18	608	16	702	18
827	20	481	31	766	23	599	16	702	18
817	18	481	31	707	21	744	17	810	18
827	15	660	29	665	22	739	19	769	18
825	15	631	29	628	25	672	21	672	21
830	14	687	23	588	23	562	20	681	20
812	14	700	23	536	29	531	21	667	21
799	11	687	23	520	29	708	23	663	23
771	10	837	15	551	29	687	24	663	23
802	13	849	15	528	29	654	25	633	24
786	12	837	15	547	20	667	25	609	25
802	13	848	14	549	29	614	31	613	26
792	12	837	14	534	29	600	31	651	27
812	14	838	14	551	29	597	31	812	14
809	12	837	15	527	29	600	31	812	14
802	13	847	13	458	30				
825	12	847	13	534	29				
802	13	847	13	546	29				
802	13	840	13	512	29				
812	14	837	14	541	29				

Instance p44r									
Reward_WAM	P_nodes_WAM	Reward_POWAM	P_nodes_POWAM	Reward_EMM	P_nodes_EMM	Reward_ECPM	P_nodes_ECPM	Reward_ECSCM	P_nodes_ECSCM
604	31	570	31	989	22	572	18	861	23
887	27	636	31	918	23	901	21	861	23
887	27	636	31	871	28	902	22	861	23
903	28	613	33	830	29	901	21	861	23
943	20	825	29	777	30	900	22	861	23
948	21	833	29	759	29	748	24	918	22
965	21	900	26	735	29	719	25	744	26
947	17	833	29	680	28	751	29	734	24
947	22	900	26	592	31	819	30	796	26
946	18	900	26	545	31	819	30	788	26
951	16	894	23	587	31	867	28	751	27
947	17	902	24	594	31	888	31	703	28
951	16	881	24	561	31	863	30	732	29
947	17	930	17	532	31	834	21	649	30
972	17	931	19	576	31			947	17
947	17	933	22	647	31				
947	17	909	21	625	31				
947	17	916	20	641	31				
954	17	918	19	579	31				
947	17	900	23	625	31				
947	17	923	17	513	31				

Table 2. Numerical results of instances p54q and p54r.

Instance p54q									
Reward_WAM	P_nodes_WAM	Reward_POWAM	P_nodes_POWAM	Reward_EMM	P_nodes_EMM	Reward_ECPM	P_nodes_ECPM	Reward_ECSCM	P_nodes_ECSCM
535	19	535	19	795	12	645	14	640	13
795	12	580	19	795	12	695	13	635	13
795	12	570	19	725	14	690	14	630	14
795	12	580	19	740	14	675	15	620	15
795	12	580	19	645	15	650	18	590	16
795	12	580	19	600	16	650	18	595	17
790	12	680	16	570	19	650	18	595	18
795	12	755	14	535	19	600	20	580	19
795	12	785	12	535	19				
780	11	795	12	535	19				
795	12	785	12	535	19				
795	12	785	12	535	19				
775	11	785	11	535	19				
795	12	785	12	535	19				
770	12	785	12	535	19				
770	12	770	12	535	19				
795	12	770	12	535	19				
770	10	785	11	535	19				
770	10	780	10	535	19				
795	12	780	11	535	19				
795	12	785	12	535	19				

Instance p54r									
Reward_WAM	P_nodes_WAM	Reward_POWAM	P_nodes_POWAM	Reward_EMM	P_nodes_EMM	Reward_ECPM	P_nodes_ECPM	Reward_ECSCM	P_nodes_ECSCM
670	20	665	20	855	12	750	12	730	12
775	18	715	20	815	15	725	11	710	13
840	15	715	20	780	17	740	12	710	15
850	14	715	20	730	19	725	14	710	16
860	11	715	20	725	20	735	15	640	16
855	12	755	19	665	20	715	15	630	18
860	11	755	19	705	20	705	16	670	19
855	12	765	18	575	19	775	17	670	20
855	13	765	19	625	20	860	10	855	12
860	9	780	17	625	20	860	10		
865	10	860	14	630	20	860	10		
855	12	855	14	655	20				
865	10	845	14	670	20				
860	11	860	12	630	20				
860	11	850	13	670	20				
855	12	850	14	625	20				
860	10	855	11	630	20				
850	11	860	11	625	20				
855	9	855	11	625	20				
860	9	855	13	670	20				
865	10	865	11	625	20				

Table 3. Numerical results of instances p74q and p74r.

Instance p74q									
Reward_WAM	P_nodes_WAM	Reward_POWAM	P_nodes_POWAM	Reward_EMM	P_nodes_EMM	Reward_ECPM	P_nodes_ECPM	Reward_ECSM	P_nodes_ECSM
496	20	377	23	742	15	708	17	699	17
704	16	533	20	702	16	708	17	699	17
700	14	534	20	685	17	689	15	699	17
700	14	655	18	630	17	632	17	699	17
700	14	655	18	628	18	653	19	699	17
697	14	687	17	591	20	638	18	675	18
733	13	655	18	591	20	626	19	665	19
733	13	689	17	584	20	640	20	733	13
733	13	687	17	619	20				
733	13	687	17	607	20				
733	13	689	17	607	20				
733	13	698	16	607	20				
733	13	698	16	591	20				
733	13	701	15	607	20				
733	13	701	15	607	20				
733	13	711	12	607	20				
733	13	748	13	607	20				
733	13	739	12	607	20				
733	13	742	13	607	20				
733	13	747	13	584	20				

Instance p74r									
Reward_WAM	P_nodes_WAM	Reward_POWAM	P_nodes_POWAM	Reward_EMM	P_nodes_EMM	Reward_ECPM	P_nodes_ECPM	Reward_ECSM	P_nodes_ECSM
592	22	377	23	702	16	705	15	672	16
690	21	533	20	670	16	688	17	702	15
693	12	534	20	643	21	709	14	688	17
693	12	655	18	653	19	678	17	688	17
693	12	655	18	562	19	677	17	688	17
698	11	687	17	627	22	691	17	691	17
698	11	655	18	627	22	530	18	530	18
698	11	689	17	593	22	619	17	737	17
700	10	687	17	580	22	595	19	704	18
698	9	687	17	588	22	579	19	690	21
705	12	689	17	588	22	593	20	700	10
700	10	698	16	627	22	700	10	700	10
700	12	698	16	592	22	700	10	700	10
700	10	698	16	588	22				
693	12	701	15	588	22				
702	10	701	15	588	22				
700	10	711	12	588	22				
700	10	748	13	588	22				
705	9	739	12	588	22				
705	9	742	13	485	22				
700	10	747	13	588	22				

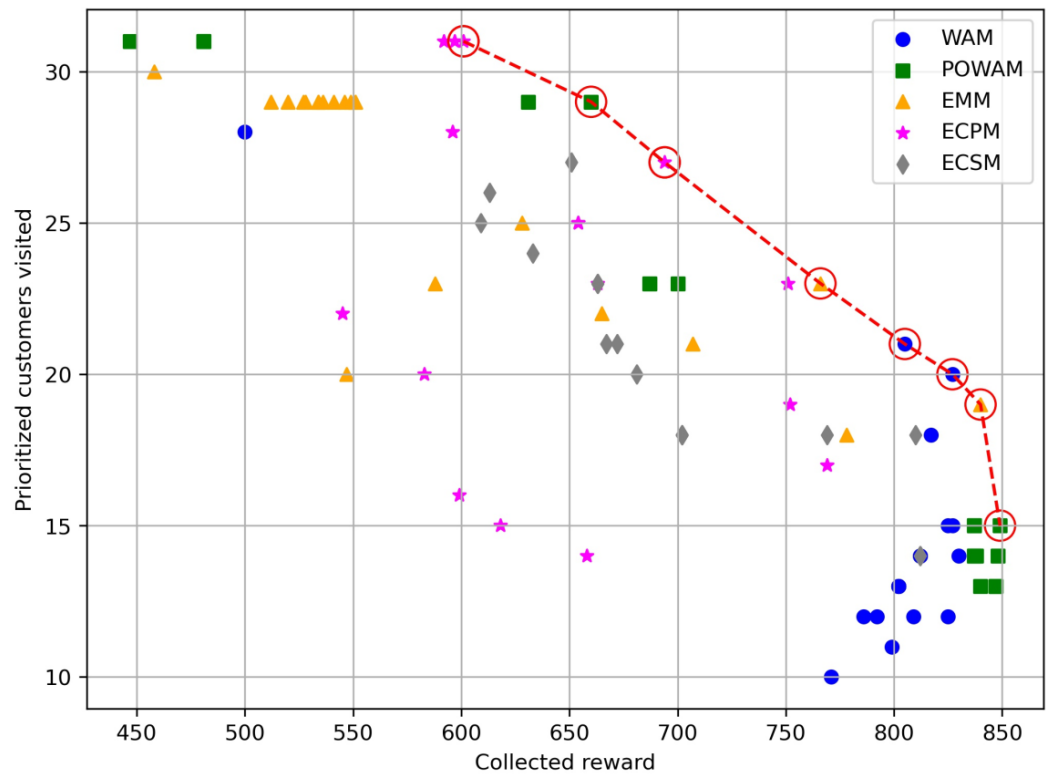


Figure 4. Pareto frontier for the MO-TOP p44o.

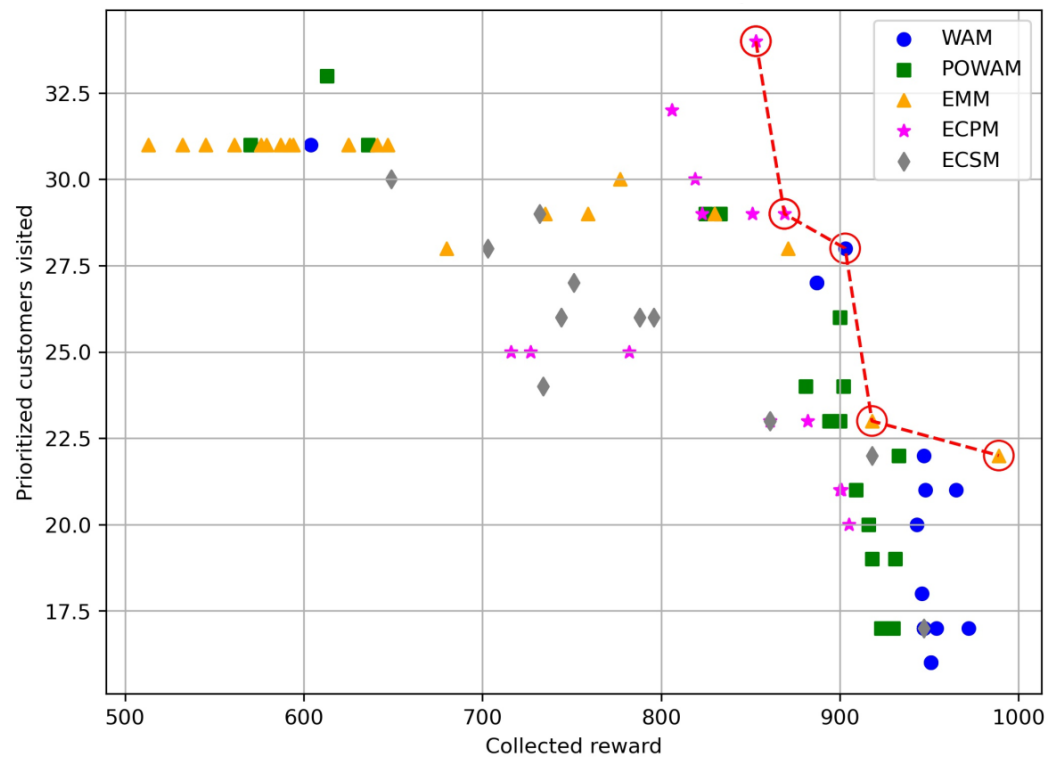


Figure 5. Pareto frontier for the MO-TOP p44r.

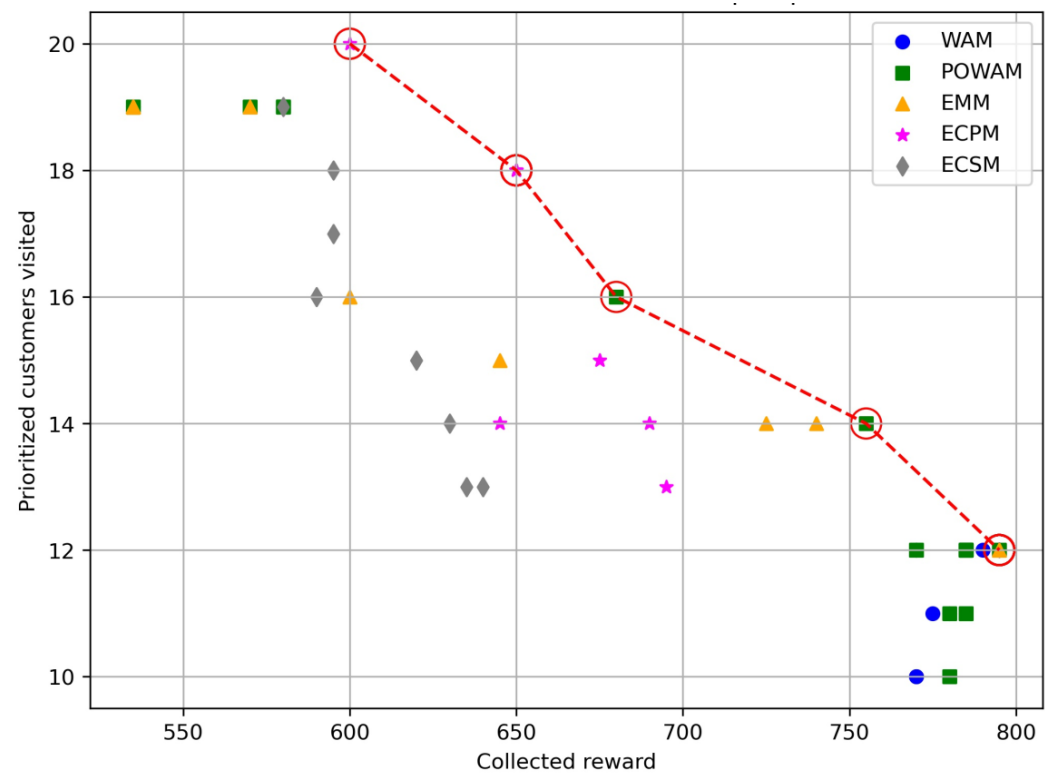


Figure 6. Pareto frontier for the MO-TOP p54q.

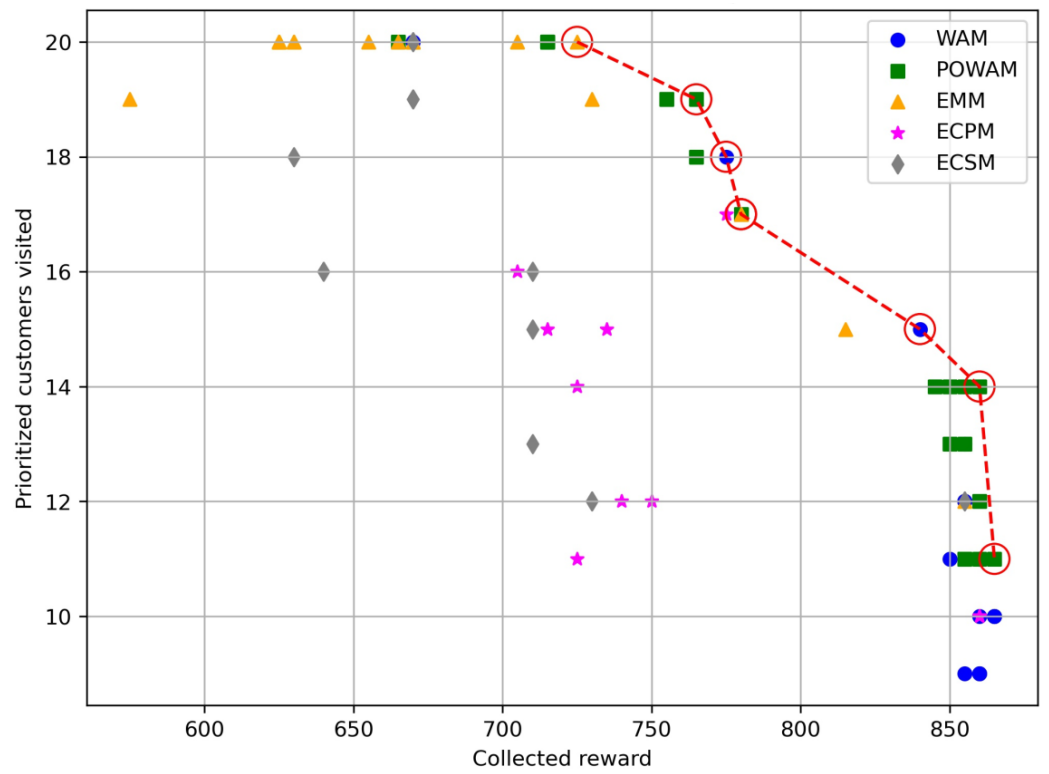


Figure 7. Pareto frontier for the MO-TOP p54r.

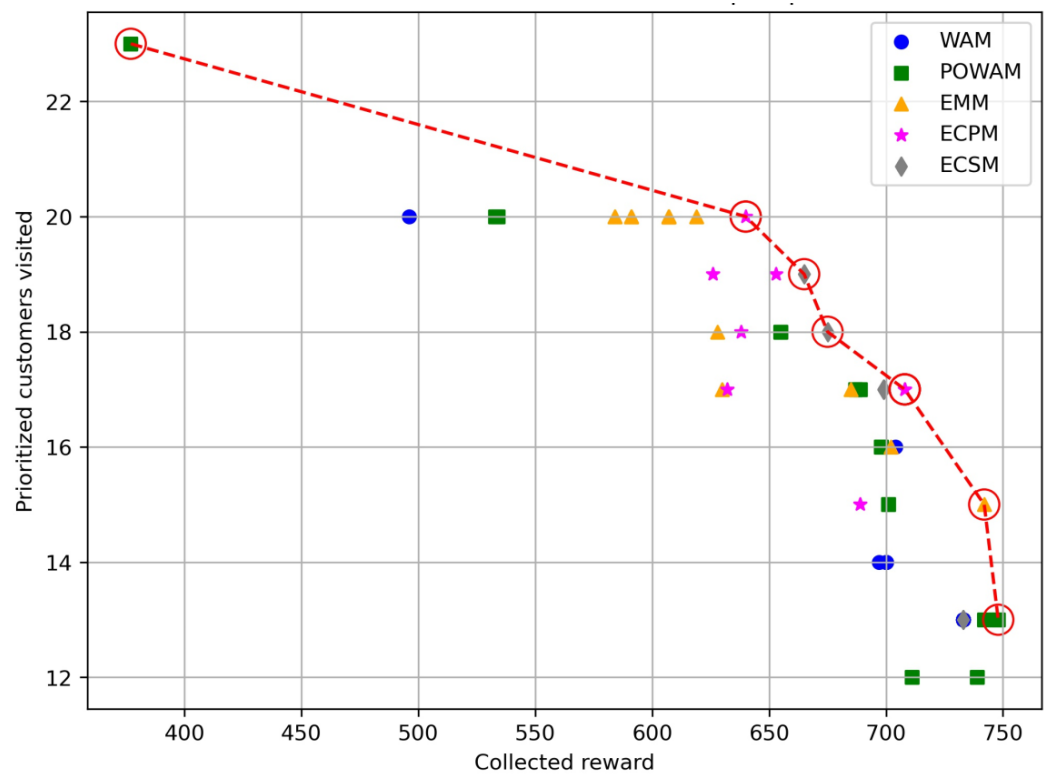


Figure 8. Pareto frontier for the MO-TOP p74q.

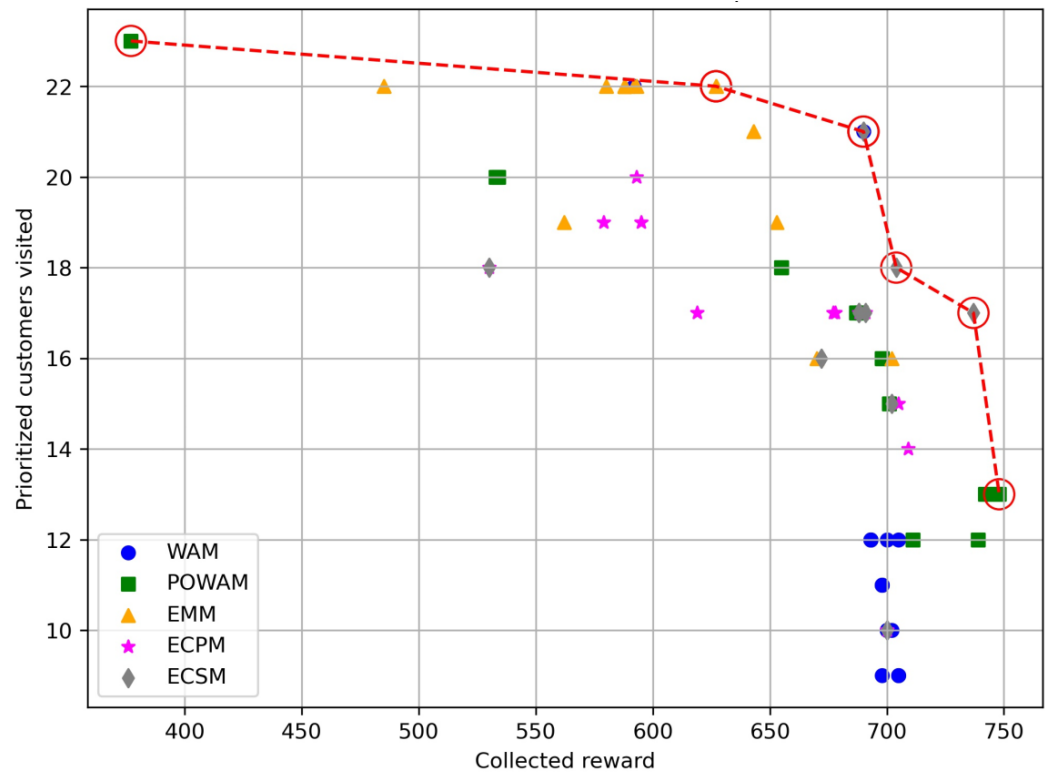


Figure 9. Pareto frontier for the MO-TOP p74r.

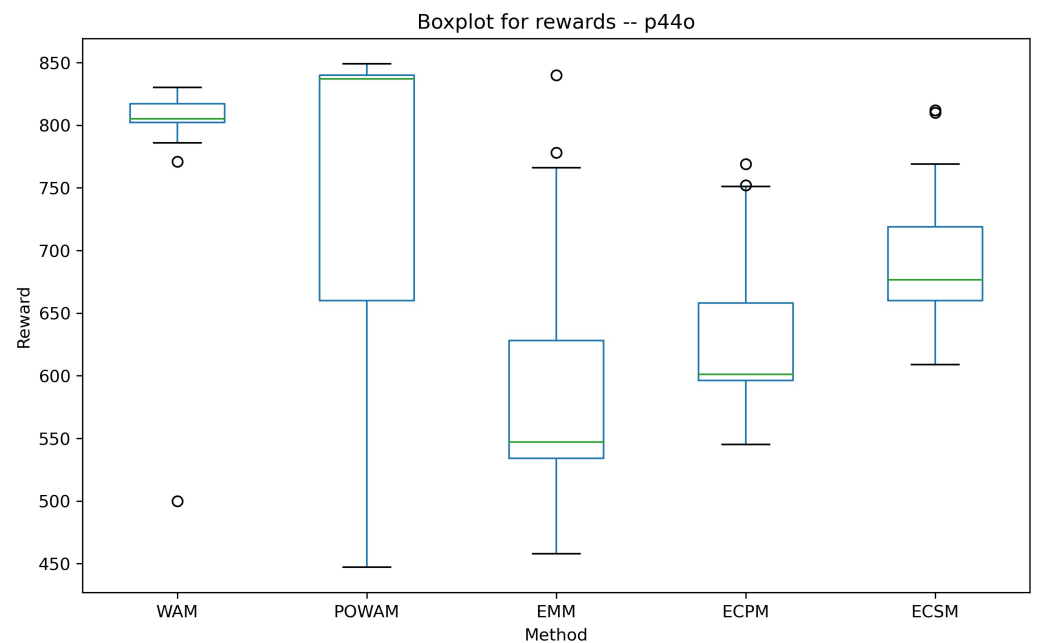


Figure 10. Solutions for the MO-TOP p44o using all the described methods for rewards.

It can be observed that there are some methods whose solutions offer more variability compared with the others. This tool is intended to assist the customer’s decision making in choosing which method to use for the resolution of their particular problem, depending on whether they want to obtain a wider range of solutions or not. We can observe in Figure 10 that the medians are very close to the first or third quartile, depending on the method. However, for the boxplot of priority nodes (Figure 11), a more balanced distribution is observed for the WAM, ECPM, and ECSM.

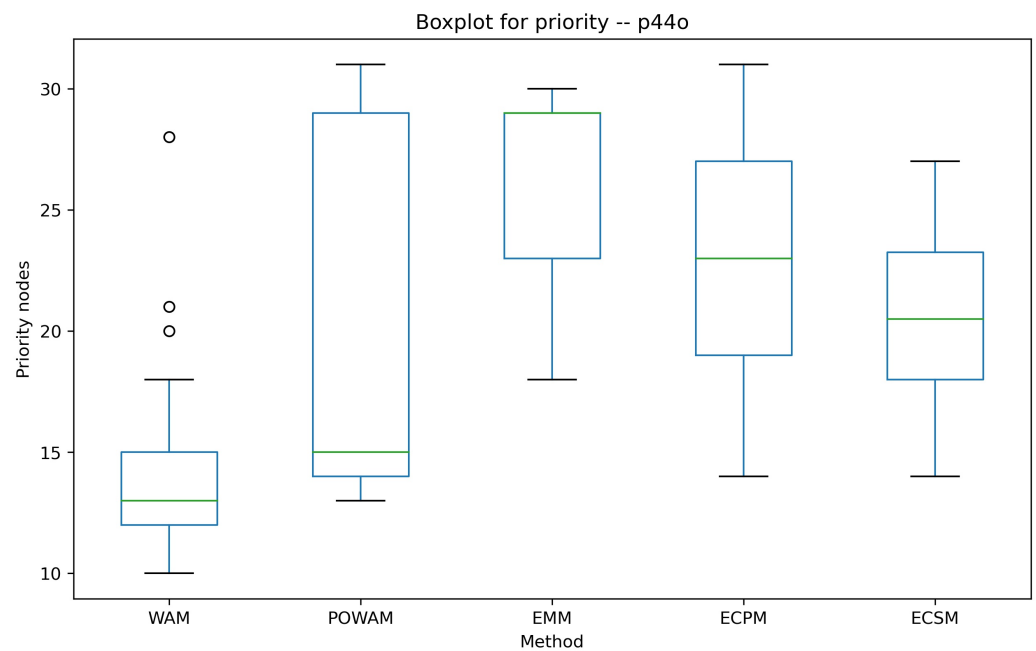


Figure 11. Solutions for the MO-TOP p44o using all the described methods for priority nodes visited.

6. Conclusions and Future Work

The present study has analyzed the Multiobjective Team Orienteering Problem with a focus on prioritized nodes. Several distinct multiobjective optimization methodologies have been considered: the Weighted Average Method, the Ponderate Weighted Average Method, the epsilon-constraint method, and the Epsilon-Modified Method. This paper compares their efficacy in maximizing rewards obtained from visited nodes while optimizing the total number of prioritized nodes visited. In order to carry this out, a series of computational experiments on an extended version of popular TOP instances has been carried out. The Pareto frontiers generated by these methodologies illustrate the inherent trade-offs between the rewards accrued and the number of prioritized nodes visited, providing decision-makers with a spectrum of solutions catering to varying preferences and constraints.

The Weighted Average Method and its weighted counterpart POWAM demonstrated their aptitude in providing solutions with distinct trade-offs between the number of prioritized nodes visited and the rewards obtained. The POWAM, in particular, exhibited greater variability in solutions, offering a range of possibilities for decision-makers to explore based on their objectives. In parallel, the epsilon-constraint method introduced a constraint-based approach, allowing for the exploration of solutions where one objective was maximized while the other stayed within predefined epsilon values. Finally, the Epsilon-Modified Method maximized both values, adding a new relaxed constraint depending on epsilon. These methods showcased alternative solutions based on epsilon values, presenting a diversified set of trade-offs between rewards and prioritized nodes visited. A weighting factor of $\lambda = 0.1$ has been employed in this study, demonstrating the effectiveness of reward weighting in samples with high rewards. An area worth exploring further would be the utilization of variable weighting factors tailored to the characteristics of the data in each example. Additionally, investigating how to incorporate this reward weighting into the ECM and EMM algorithms could be beneficial. Our comparative analysis signifies that the choice of the most suitable method for addressing the MO-TOP with prioritized nodes is contingent upon the decision-makers' specific preferences, goals, and constraints. Each method has distinct strengths and trade-offs, offering a range of solutions that cater to different optimization priorities.

This paper focuses on the deterministic version of the MultiObjective TOP, considering a generalization where the time of movement along each edge is invariant and is given by the Euclidean distance. Considering a more realistic scenario, this MO-TOP can be

specified to use dynamic time, in which the travel time of each vehicle is measured in real time, allowing the incorporation of unexpected events. Some research lines that can be explored further are the following ones: (i) the integration of machine learning techniques, such as reinforcement learning, with traditional optimization algorithms could offer novel approaches to solve dynamic instances of the MO-TOP; (ii) addressing practical constraints, such as time windows, traffic congestion, vehicle capacities, and dynamic node prioritization, can render the models more applicable to real-world scenarios, making solutions more feasible and adaptable; (iii) evaluating the applicability of MO-TOP models in diverse sectors such as logistics, transportation, emergency response, and telecommunications can provide valuable insights into specific use case scenarios, enabling tailored solutions for real-world challenges; and (iv) the consideration of environmental impacts, such as reducing carbon emissions or optimizing routes for energy efficiency, could be integrated into MO-TOP models to address sustainability concerns.

Author Contributions: Conceptualization, A.A.J., L.A.-A. and S.O.-C.; methodology, L.A.-A., N.G. and S.O.-C.; software, A.A.J., L.A.-A., N.G. and S.O.-C.; formal analysis, L.A.-A. and N.G.; writing—original draft preparation, L.A.-A., S.O.-C., A.L. and N.G.; writing—review and editing, A.A.J. All authors have read and agreed to the published version of the manuscript.

Funding: This work has been partially funded by the Spanish Ministry of Science and Innovation (PID2022-138860NB-I00 and RED2022-134703-T).

Institutional Review Board Statement: Not applicable.

Informed Consent Statement: Not applicable.

Data Availability Statement: All required data is contained in the manuscript.

Conflicts of Interest: The authors declare no conflicts of interest.

Nomenclature

N	Set of intermediate nodes: $i, j \in N = 1, 2, \dots, n$
N'	Set of nodes including the initial and final depots: $N' = 0, 1, 2, \dots, n + 1$
E	Set of edges connecting the nodes: $E = (i, j) / i, j \in N', i \neq j$
G	Graph of the network, $G = (N', E)$
D	Set of homogeneous vehicles $d \in D$
t_{ij}	Travel time for each edge, $t_{ij} = t_{ji} > 0, \forall i, j \in N$
t_{max}	Maximum travel time for each vehicle or route
u_i	Reward of the node $i \in N$
x_{ij}^d	Binary variable whose value is equal to 1 if vehicle d traverses edge (i, j)
y_i^d	Position of the node i in the tour made for the vehicle d
z_i	Binary variable whose value is equal to 1 if node i is priority
λ	Weight for pondering the rewards in the biobjective function
α	Convex linear combination constant in the efficiency value
γ	Convex linear combination constant in the biefficiency value
η	Convex linear combination constant in the biobjective function
s_{ij}	Time-based savings associated to the edge (i, j) , $s_{ij} = t_{i(n+1)} + t_{0j} - t_{ij}$
e_{ij}	Efficiency value associated to the edge (i, j) , $e_{ij} = \alpha s_{ij} + (1 - \alpha)(u_i + u_j)$
b_{ij}	Biefficiency value associated to the edge (i, j) , $b_{ij} = \gamma e_{ij} + (1 - \gamma)(z_i + z_j)$
ε	Deviation from the optimal value for the secondary objectives, $\varepsilon > 0$
PN^*	Total number of priority nodes being visited

References

1. Chao, I.M.; Golden, B.L.; Wasil, E.A. The team orienteering problem. *Eur. J. Oper. Res.* **1996**, *88*, 464–474. [[CrossRef](#)]
2. Golden, B.L.; Levy, L.; Vohra, R. The orienteering problem. *Nav. Res. Logist.* **1987**, *34*, 307–318. [[CrossRef](#)]
3. Gunawan, A.; Lau, H.C.; Vansteenwegen, P. Orienteering Problem: A survey of recent variants, solution approaches and applications. *Eur. J. Oper. Res.* **2016**, *255*, 315–332. [[CrossRef](#)]

4. Gunawan, A.; Ng, K.M.; Kendall, G.; Lai, J. An iterated local search algorithm for the team orienteering problem with variable profits. *Eng. Optim.* **2018**, *0273*, 1–16. [[CrossRef](#)]
5. Vansteenwegen, P.; Souffriau, W.; Van Oudheusden, D. The orienteering problem: A survey. *Eur. J. Oper. Res.* **2011**, *209*, 1–10. [[CrossRef](#)]
6. Panadero, J.; Juan, A.A.; Bayliss, C.; Currie, C. Maximising reward from a team of surveillance drones: A simheuristic approach to the stochastic team orienteering problem. *Eur. J. Ind. Eng.* **2020**, *14*, 485–516. [[CrossRef](#)]
7. Gosavi, A. *Simulation-Based Optimization*; Springer: Berlin/Heidelberg, Germany, 2015.
8. Archetti, C.; Hertz, A.; Speranza, M.G. Metaheuristics for the team orienteering problem. *J. Heuristics* **2007**, *13*, 49–76. [[CrossRef](#)]
9. Ke, L.; Archetti, C.; Feng, Z. Ants can solve the team orienteering problem. *Comput. Ind. Eng.* **2008**, *54*, 648–665. [[CrossRef](#)]
10. Vansteenwegen, P.; Souffriau, W.; Berghe, G.V.; Van Oudheusden, D. A guided local search metaheuristic for the team orienteering problem. *Eur. J. Oper. Res.* **2009**, *196*, 118–127. [[CrossRef](#)]
11. Vansteenwegen, P.; Souffriau, W.; Berghe, G.V.; Van Oudheusden, D. Iterated local search for the team orienteering problem with time windows. *Comput. Oper. Res.* **2009**, *36*, 3281–3290. [[CrossRef](#)]
12. Souffriau, W.; Vansteenwegen, P.; Berghe, G.V.; Van Oudheusden, D. A path relinking approach for the team orienteering problem. *Comput. Oper. Res.* **2010**, *37*, 1853–1859. [[CrossRef](#)]
13. Tricoire, F.; Romauch, M.; Doerner, K.F.; Hartl, R.F. Heuristics for the multi-period orienteering problem with multiple time windows. *Comput. Oper. Res.* **2010**, *37*, 351–367. [[CrossRef](#)]
14. Souffriau, W.; Vansteenwegen, P.; Vanden Berghe, G.; Van Oudheusden, D. The multiconstraint team orienteering problem with multiple time windows. *Transp. Sci.* **2013**, *47*, 53–63. [[CrossRef](#)]
15. Verbeeck, C.; Sörensen, K.; Aghezzaf, E.H.; Vansteenwegen, P. A fast solution method for the time-dependent orienteering problem. *Eur. J. Oper. Res.* **2014**, *236*, 419–432. [[CrossRef](#)]
16. Vidal, T.; Maculan, N.; Ochi, L.S.; Vaz Penna, P.H. Large neighborhoods with implicit customer selection for vehicle routing problems with profits. *Transp. Sci.* **2016**, *50*, 720–734. [[CrossRef](#)]
17. Paolucci, M.; Anghinolfi, D.; Tonelli, F. Field services design and management of natural gas distribution networks: A class of vehicle routing problem with time windows approach. *Int. J. Prod. Res.* **2018**, *56*, 1154–1170. [[CrossRef](#)]
18. Estrada-Moreno, A.; Ferrer, A.; Juan, A.A.; Panadero, J.; Bagirov, A. The Non-Smooth and Bi-Objective Team Orienteering Problem with Soft Constraints. *Mathematics* **2020**, *8*, 1461. [[CrossRef](#)]
19. Ruiz-Meza, J.; Brito, J.; Montoya-Torres, J.R. A GRASP to solve the multi-constraints multi-modal team orienteering problem with time windows for groups with heterogeneous preferences. *Comput. Ind. Eng.* **2021**, *162*, 107776. [[CrossRef](#)]
20. Sankaran, P.; McConky, K.; Sudit, M.; Ortiz-Peña, H. GAMMA: Graph attention model for multiple agents to Solve team orienteering problem With multiple depots. *IEEE Trans. Neural Netw. Learn. Syst.* **2022**, *34*, 9412–9423. [[CrossRef](#)]
21. Panadero, J.; Juan, A.A.; Ghorbani, E.; Faulin, J.; Pagès-Bernaus, A. Solving the stochastic team orienteering problem: Comparing simheuristics with the sample average approximation method. *Int. Trans. Oper. Res.* **2023**. [[CrossRef](#)]
22. Wattanasang, N.; Ransikarbum, K. Model and Analysis of Economic- and Risk-Based Objective Optimization Problem for Plant Location within Industrial Estates Using Epsilon-Constraint Algorithms. *Computation* **2021**, *9*, 46. [[CrossRef](#)]
23. Mohammadi, T.; Sajadi, S.M.; Najafi, S.E.; Taghizadeh-Yazdi, M. Multi Objective and Multi-Product Perishable Supply Chain with Vendor-Managed Inventory and IoT-Related Technologies. *Mathematics* **2024**, *12*, 679. [[CrossRef](#)]
24. Nikoubin, A.; Mahnam, M.; Moslehi, G. A relax-and-fix Pareto-based algorithm for a bi-objective vaccine distribution network considering a mix-and-match strategy in pandemics. *Appl. Soft Comput.* **2023**, *132*, 109862. [[CrossRef](#)]
25. Shojatalab, G.; Nasseri, S.H.; Mahdavi, I. New multi-objective optimization model for tourism systems with fuzzy data and new algorithm for solving this model. *Oper. Res. Soc. India* **2022**, *59*, 1018–1037. [[CrossRef](#)]
26. Elmi, Z.; Li, B.; Liang, B.; Lau, Y.; Borowska-Stefańska, M.; Wiśniewski, S.; Dulebenets, M.A. An epsilon-constraint-based exact multi-objective optimization approach for the ship schedule recovery problem in liner shipping. *Comput. Ind. Eng.* **2023**, *183*, 109472. [[CrossRef](#)]
27. Banerjee, A.; Pradhan, S.; Misra, B.; Chakraborty, S. A Guide to Meta-Heuristic Algorithms for Multi-objective Optimization: Concepts and Approaches. In *Applied Multi-Objective Optimization*; Springer Nature: Singapore, 2024; pp. 1–19.
28. Memarian, S.; Behmanesh-Fard, N.; Aryai, P.; Shokouhifar, M.; Mirjalili, S.; Romero-Ternero, M. TSFIS-GWO: Metaheuristic-driven takagi-sugeno fuzzy system for adaptive real-time routing in WBANs. *Appl. Soft Comput.* **2024**, *155*, 111427. [[CrossRef](#)]
29. Evers, L.; Glorie, K.; van der Ster, S.; Barros, A.I.; Monsuur, H. A two-stage approach to the orienteering problem with stochastic weights. *Comput. Oper. Res.* **2014**, *43*, 248–260. [[CrossRef](#)]
30. Estrada-Moreno, A.; Savelsbergh, M.; Juan, A.A.; Panadero, J. Biased-randomized iterated local search for a multiperiod vehicle routing problem with price discounts for delivery flexibility. *Int. Trans. Oper. Res.* **2019**, *26*, 1293–1314. [[CrossRef](#)]
31. Panadero, J.; de Armas, J.; Currie, C.S.; Juan, A.A. A simheuristic approach for the stochastic team orienteering problem. In Proceedings of the 2017 Winter Simulation Conference (WSC), Las Vegas, NV, USA, 3–6 December 2017; pp. 3208–3217.

Disclaimer/Publisher’s Note: The statements, opinions and data contained in all publications are solely those of the individual author(s) and contributor(s) and not of MDPI and/or the editor(s). MDPI and/or the editor(s) disclaim responsibility for any injury to people or property resulting from any ideas, methods, instructions or products referred to in the content.